

Learning-Based Conformal Tube MPC for Safe Control in Interactive Multi-Agent Systems

Shuqi Wang, Yue Gao and Xiang Yin

Abstract—Safety assurance in multi-agent systems with coupled dynamics is a fundamental yet challenging problem, especially when agents exhibit uncertain and state-dependent behaviors. Classical robust control often assumes worst-case disturbances, leading to overly conservative actions. In this work, we propose a learning-based framework that combines conformal prediction with model predictive control (MPC) to ensure probabilistic safety under action-level uncertainty. Unlike prior approaches that predict future states, we directly model the control action of the uncontrollable agent as a stochastic function of the joint state, trained via neural networks and calibrated using conformal prediction. This enables us to construct dynamic, probabilistically guaranteed reachable tubes for the uncontrollable agent. These tubes are then embedded into an MPC formulation to synthesize control actions for the controllable agent that ensure safe interactions over a finite planning horizon. We provide formal stepwise and cumulative safety guarantees, and demonstrate the effectiveness of our approach through a pedestrian-vehicle interaction scenario. Compared to baseline methods, our framework achieves higher safety rates while maintaining high performance in terms of speed and responsiveness.

I. INTRODUCTION

Safety is a fundamental requirement for autonomous systems operating in dynamic, uncertain environments such as autonomous driving, human-robot interaction, and multi-agent coordination. These systems must make real-time decisions while ensuring safe behavior, even in the presence of other agents whose actions are not directly controllable [1], [2]. For instance, in autonomous driving, the ego vehicle must continuously monitor its surroundings to ensure the safety of itself, pedestrians, and other vehicles [3].

To achieve safe control in real-world scenarios, it is essential to account for the presence of uncontrollable agents in the environment [4]. A particular challenge arises when these environments involve *coupled agents*, where the future behavior of an uncontrollable agent depends on the state and actions of the controllable system [5], [6]. For example, a pedestrian may slow down or change direction in response to an approaching vehicle. Such coupling significantly complicates both prediction and planning, as the joint evolution of agents is no longer independent.

Another difficulty lies in the fact that the internal decision-making process of uncontrollable agents is unobservable. Classical robust control techniques typically assume worst-case disturbances [7], [8], which often lead to overly con-

servative behavior and poor scalability in interactive contexts. Some stochastic control frameworks, such as model predictive control with chance constraints [9], model the behavior of external agents as stochastic processes to provide probabilistic safety guarantees. However, the true distribution governing these behaviors is generally unknown and difficult to model analytically.

More recently, data-driven approaches have emerged, in which neural networks are trained on real-world trajectory data to predict the future behavior of other agents [10], [11], [12]. While powerful, such predictors typically do not provide calibrated uncertainty estimates, making them risky to use directly in safety-critical control pipelines. Without reliable uncertainty quantification, it is difficult to make guarantees about the safety of the resulting decisions. In response to this gap, there has been growing interest in integrating *distribution-free uncertainty quantification* methods such as *conformal prediction* into planning and control. Conformal prediction allows one to wrap any black-box predictor with statistical guarantees on the prediction error, under mild assumptions [13]. This makes it a promising tool for building safe control frameworks that leverage data-driven models while retaining formal safety assurances [14], [15].

In this work, we propose a new safe control framework for systems with coupled agent dynamics, where uncertainty arises at the action level of the uncontrollable agent. Rather than predicting future states, we model the agent's action as a random variable drawn from an unknown, state-dependent distribution, conditioned on the current joint state. This distribution is learned from data via a neural network and calibrated using conformal prediction, yielding finite-sample probabilistic guarantees on prediction regions. We integrate these action-level uncertainty sets into a dynamic reachable tube construction. At each time step, we compute the multi-step reachable set of the uncontrollable agent based on the conformal action region, and embed the result into a model predictive control (MPC) formulation. This enables the controllable agent to optimize its trajectory while ensuring that the joint state remains within a user-defined safety set with high probability over the planning horizon. This framework is particularly well-suited for real-time decision-making in interactive and perception-uncertain environments such as urban driving, warehouse robotics, or assistive robotics. It bridges offline conformal prediction with robust reachability-based planning, enabling high-confidence safety guarantees in complex multi-agent scenarios.

Related Works Conformal prediction (CP) has been used widely in the past years in safe control problem.

This work was supported by the National Natural Science Foundation of China (62173226, 62061136004).

Shuqi Wang, Yue Gao and Xiang Yin are with School of Automation and Intelligent Sensing, Shanghai Jiao Tong University, Shanghai 200240, China. e-mail: {wangshuqi, yuegao, yinxiang}@sjtu.edu.cn.

In [16], CP has been applied to the output of a neural state estimator that processes uncertain perception signals. The resulting CP region was then used to guide a control barrier function (CBF)-based safety controller. Related efforts such as [17] and [18] studied how neural networks propagate error through time in the form of reachable sets. However, these works focus on the uncertainty quantification in the perception module. In our work, we assume perfect state observation, but aim to quantify and control the uncertainty arising from the future behavior of uncontrollable agents whose actions are coupled with the controllable agent.

In the context of using conformal prediction (CP) for safe control in the presence of uncontrollable agents, [15] proposed a framework that integrates CP into a model predictive control framework. However, their method assumes that the future behavior of dynamic agents follows a stationary distribution that is independent of the controllable system's state—an assumption that does not hold in many interactive scenarios. To address this limitation, [19] proposed an adaptive conformal prediction (ACP) framework that recalibrates uncertainty online along each trajectory. By integrating ACP into MPC, their method adapts prediction regions to changes in agent behavior across episodes and exhibits improved robustness under distribution shift. In particular, it does not capture how the behavior of an uncontrollable agent may change within each episode in response to the actions of the controllable agent, leading to interaction-induced distribution shifts.

Our work proposes a reachability-based MPC framework that explicitly models the coupled dynamics between controllable and uncontrollable agents. We represent the uncontrollable agent's action as a random variable conditioned on the joint state, and learn this action-level distribution from offline simulated data. Using conformal prediction, we calibrate this distribution to obtain region-specific, finite-sample uncertainty bounds. These bounds are then used to construct worst-case dynamic reachable tubes over the planning horizon. Embedding these tubes into MPC enables long-term planning with provable safety guarantees, offering higher safety confidence than online adaptive methods.

II. PRELIMINARY AND PROBLEM FORMULATION

A. System Models

In this work, we consider a scenario where a controlled system operates in an environment with a single uncontrollable agent. We assume that the dynamics of both systems are known, but the control law of the uncontrollable agent is unknown. Our objective is to design a control law for the controlled system to ensure safety. For simplicity, we consider a single-agent setting for both the controlled and uncontrollable systems. Note that our approach can be easily extended to multi-agent scenarios.

Controlled System: We model the controllable agent by a discrete-time nonlinear system

$$x_{k+1} = f(x_k, u_k), \quad (1)$$

where $x_k \in \mathbb{X} \subseteq \mathbb{R}^{n_x}$ denotes the system state, $u_k \in \mathbb{R}^{n_u}$ is the control input, and $f : \mathbb{R}^{n_x} \times \mathbb{R}^{n_u} \rightarrow \mathbb{R}^{n_x}$ represents the dynamics of the system. Here, we assume that f of the controlled system is perfectly known and its state x_k is fully observable. Furthermore, the system dynamic is considered to be deterministic. Therefore, given an initial state and a sequence of control inputs, the future trajectory of the controlled system can be predicted perfectly in an open-loop fashion.

Uncontrollable Agent: The uncontrollable agent is also modeled by a discrete-time system

$$y_{k+1} = g(y_k, a_k), \quad (2)$$

where $y_k \in \mathbb{Y} \subseteq \mathbb{R}^{n_y}$ is the agent state, $a_k \in \mathbb{R}^{n_a}$ is the control input, and $g : \mathbb{R}^{n_y} \times \mathbb{R}^{n_a} \rightarrow \mathbb{R}^{n_y}$ is the agent dynamic, which is also assumed to be deterministic and known.

However, the behavior of the uncontrollable agent is coupled with the controlled one via its control law. Specifically, we assume that the control input of the uncontrollable agent follows an *unknown distribution* conditioned on the current states of the controllable agent x_k and the uncontrollable agent itself, i.e.,

$$a_k \sim \mathcal{D}(x_k, y_k). \quad (3)$$

This setting, where the system dynamics are known but the control policy of the external agent is unknown, arises naturally in many practical scenarios. For instance, in autonomous driving, the dynamics of surrounding vehicles can often be well-characterized, whereas the control policies of human drivers are far more challenging to model accurately due to their complex and unpredictable nature. Overall, the behavior of the uncontrollable agent is a stochastic process that depends on the trajectory of the controlled system.

B. Problem Formulation

Notations: We denote \mathbb{R}, \mathbb{N} , and \mathbb{R}^n as the set of real numbers, natural numbers, and real vectors, respectively. For a vector $v \in \mathbb{R}^n$, let $|v|$, $\|v\|$ denote its ℓ_1 -norm, and Euclidean norm. For a finite set D , let $|D|$ denote its cardinality.

Let $\mathcal{S}_{\text{safe}} \subseteq \mathbb{R}^{n_x} \times \mathbb{R}^{n_y}$ be a *safe region*, for instance, the set of states where the inter-agent distance exceeds a specified threshold. Our goal is to design a feedback control law that formally guarantees the system remains within $\mathcal{S}_{\text{safe}}$.

To achieve this, we will employ a model predictive control (MPC) framework. Specifically, at each time step, we solve an open-loop optimal control problem with built-in safety guarantees in a receding horizon fashion. This leads to the following problem formulation:

Problem 1: (Open-Loop Safe Control Problem under Coupled Uncertainty) Given the current state $(x_k, y_k) \in \mathcal{S}_{\text{safe}}$ and a reference control input sequence $\mathbf{u}_{k:k+T-1}^r \in \mathcal{U}^T$, a safe set $\mathcal{S}_{\text{safe}}$, find a control input sequence $\mathbf{u}_{k:k+T-1}^*$ that minimizes deviation from the reference control while ensuring safety with a probabilistic bound. Formally, we have

$$\mathbf{u}^* = \arg \min_{\mathbf{u} \in \mathcal{U}^T} \|\mathbf{u} - \mathbf{u}^r\|^2 \quad (4)$$

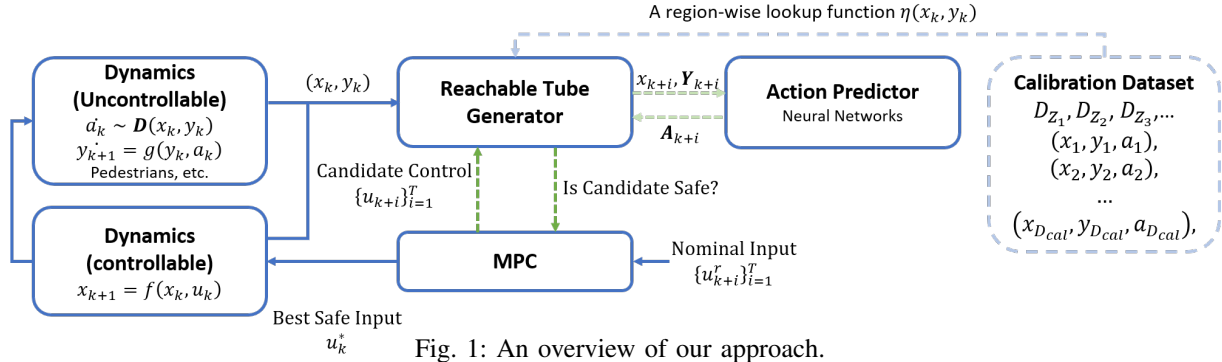


Fig. 1: An overview of our approach.

subject to, for all $i = 1, \dots, T$:

$$\begin{aligned} \mathbb{P}[(x_{k+i}, y_{k+i}) \in \mathcal{S}_{\text{safe}}] &\geq \gamma, \\ x_k &\text{ satisfies the dynamics of (1),} \\ y_k &\text{ satisfies the dynamics of (2).} \end{aligned}$$

That is, we aim to ensure that the probability of entering an unsafe state due to the uncontrollable agent remains below a threshold of $1 - \gamma$ at each time instant.

C. Data Collection and Predictor Design

To address the challenge of the unknown control law governing the uncontrollable agent, we assume access to a set of historical trajectories capturing the joint behavior of both the controlled and uncontrollable systems. Let $[x_0, x_1, \dots]$ and $[y_0, y_1, \dots]$ denote the sampled state trajectories of the controlled and uncontrollable agents, respectively. While the control actions $\{a_k\}$ of the uncontrollable agent are typically not directly observable, they can be reconstructed from the state trajectory $\{y_k\}$ given knowledge of the agent's dynamics and suitable invertibility assumptions. Thus, we further assume that a sampled control input sequence $[a_0, a_1, \dots]$ is available for our analysis.

Data Collections. We assume that we have access to \bar{K} independent observations $\{w_k := (x_k, y_k, a_k)\}_{k=1}^{\bar{K}}$ and randomly partition these observations into calibration, training and testing sets, denoted by $D_{\text{cal}} := \{w_1, \dots, w_{|D_{\text{cal}}|}\}$, $D_{\text{train}} := \{w_{|D_{\text{cal}}|+1}, \dots, w_{|D_{\text{cal}}|+|D_{\text{train}}|}\}$, and $D_{\text{test}} := \{w_{|D_{\text{cal}}|+|D_{\text{train}}|+1}, \dots, w_{\bar{K}}\}$, respectively.

Action Predictor. To address the unknown distribution of the control input for the uncontrollable agent, we use the training set D_{train} to design a predictor to forecast the next action of the uncontrollable agent. The predictor is of the form

$$\hat{a}_k = \Omega_\theta(x_k, y_k). \quad (5)$$

Note that Ω_θ could be implemented by any predictor such as neural networks (NNs) with parameters θ .

D. Region-Based Prediction Error Bound

To ensure probabilistic safety guarantees under distributional uncertainty, we employ *conformal prediction* to quantify the uncertainty inherent in data-driven predictors. Conformal prediction was introduced in [20], [21] to obtain

valid prediction regions for complex predictive models, such as neural networks, without making assumptions on the underlying distribution or the predictive model [13], [22], [23], [24].

In general, a predictor may have different performances at different regions. To quantify the uncertainty of the predictor more precisely, for systems in (1) and (2), we partition the state space uniformly into M and N disjoint regions

$$\mathbb{X} = \mathbb{X}_1 \cup \dots \cup \mathbb{X}_M \text{ and } \mathbb{Y} = \mathbb{Y}_1 \cup \dots \cup \mathbb{Y}_N.$$

We define $\mathbb{Z} = \mathbb{X} \times \mathbb{Y} = \mathbb{Z}_1 \cup \dots \cup \mathbb{Z}_{M \times N}$ as the $M \times N$ regions in the joint state space. Accordingly, the calibration dataset is also partitioned into $M \times N$ sets depending on the state regions they long to. Formally, for each region $\mathbb{Z}_p \subseteq \mathbb{Z}$, we define

$$D_{\mathbb{Z}_p} := \{(x_k, y_k, a_k) \in D_{\text{cal}} \mid (x_k, y_k) \in \mathbb{Z}_p\}$$

as the set of calibration data that belong to this region. Let $R^{(0)}, R^{(1)}, \dots, R^{(|D_{\mathbb{Z}_p|})}$ be $|D_{\mathbb{Z}_p}| + 1$ independent and identically distributed random variables. The variable $R^{(k)}$ is usually referred to as the nonconformity score, which is defined as the prediction error $R^{(k)} = \|\hat{a}_k - a_k\|$ in our study. Note that, $R^{(1)}, \dots, R^{(|D_{\mathbb{Z}_p|})}$ have specific values that can be computed based on $D_{\mathbb{Z}_p}$, and for $0 < \gamma < 1$, we define

$$\bar{R}_{\mathbb{Z}_p} = \text{Quantile}_\gamma(R^{(1)}, \dots, R^{(|D_{\mathbb{Z}_p|})}, \infty) \quad (6)$$

as their γ -quantile, which is $\bar{R}_{\mathbb{Z}_p} = R^{(r)}$ with $r = \lceil |D_{\mathbb{Z}_p}| \cdot \gamma \rceil$. Note that $R^{(0)}$ is a random variable representing the prediction error within region \mathbb{Z}_p . Based on the standard theory of conformal predictions, we have the following results.

Lemma 1: For each region \mathbb{Z}_p and any test sample $(x, y) \in \mathbb{Z}_p$ with corresponding $R^{(0)}$, the following guarantee holds:

$$\text{Prob}(R^{(0)} \leq \bar{R}_{\mathbb{Z}_p}) \geq \gamma, \quad (7)$$

where $\bar{R}_{\mathbb{Z}_p}$ is the γ -quantile as defined in Eq. (6).

Conformal prediction implies the nonconformity score R can essentially be bounded with probability γ , within the conformal region $\bar{R}_{\mathbb{Z}_p}$. Note that here $\bar{R}_{\mathbb{Z}_p} \in \mathbb{R}^a$ is a vector for each dimension. $D_{\mathbb{Z}_p}$ satisfies $\sum_{p=1}^{M \times N} |D_{\mathbb{Z}_p}| = |D_{\text{cal}}|$. As before, for meaningful prediction regions, we require $|D_{\mathbb{Z}_p}| \geq \lceil (|D_{\mathbb{Z}_p}| + 1) \cdot \gamma \rceil$, otherwise $\bar{R}_{\mathbb{Z}_p} = \infty$.

Therefore, for an arbitrary state $(x, y) \in \mathbb{Z}$, we denote by $\mathbb{Z}_p[x, y] \subseteq \mathbb{Z}$ the corresponding region it belongs to. Then we define

$$\eta(x, y) := \bar{R}_{\mathbb{Z}_p[x, y]}. \quad (8)$$

as the conformal bound with confidence level γ . In practice, $\eta(x, y)$ is implemented as a lookup table indexed by the region \mathbb{Z}_p that contains (x, y) . This allows for efficient evaluation of the conformal bound during runtime.

Remark 1 (On Regional Calibration Validity): While Lemma 1 formally requires i.i.d. calibration data, we relax this via a two-step approximation. First, we partition the state space into disjoint regions $\mathbb{Z}_1, \mathbb{Z}_2, \dots$ and apply conformal calibration within each, following the conditional conformal prediction framework [25]. This yields approximate validity when regional data are stable and sufficient. Then, within each region, we interpret the data as drawn from a mixture of latent distributions, a common scenario in machine learning due to heterogeneous sources. While this violates strict exchangeability, conformal prediction has been shown to retain approximate coverage under mild distributional heterogeneity [26].

By Lemma 1, we have the following equivalent result.

Proposition 1: For any sample (x, y, a) in the testing set with prediction $\hat{a}(x, y) = \Omega_\theta(x, y)$, we have

$$\text{Prob}[a \in \mathcal{A}(x, y)] \geq \gamma, \quad (9)$$

where

$$\mathcal{A}(x, y) = \{a \in \mathbb{R}^{n_a} \mid \|\hat{a}(x, y) - a\| \leq \eta(x, y)\} \quad (10)$$

is the estimated conformal prediction region for the uncontrollable agent's action at state (x, y) .

III. DYNAMIC TUBE MODEL PREDICTIVE CONTROL

A. Overview of Our Approach

We propose a model predictive control (MPC) framework that ensures probabilistic safety in interactive environments involving coupled agents, where the behavior of the uncontrollable agent depends on the state and actions of the controlled system. The key idea is to explicitly account for uncertainty at the action level by combining data-driven behavior prediction, conformal calibration, and reachable set propagation into a unified control architecture.

Given the current joint state (x_k, y_k) of the controllable and uncontrollable agents, we first employ a neural network to predict the future action \hat{a}_k of the uncontrollable agent. To quantify uncertainty in the prediction, we apply conformal prediction to construct a probabilistically valid region $\mathcal{A}(x_k, y_k)$ that contains the true action a_k with a user-specified confidence level γ .

We then recursively propagate the set of possible pedestrian states over a planning horizon, using the calibrated action region $\mathcal{A}(x, y)$ at each time step. This results in a sequence of reachable sets $\mathcal{Y}_{k+1}, \dots, \mathcal{Y}_{k+T}$ representing the possible future positions of the uncontrollable agent under worst-case action uncertainty (Shown in Fig. 3).

These dynamically constructed reachable tubes are embedded into an MPC formulation that optimizes the control sequence $\mathbf{u}_{k:k+T-1}$ for the controllable agent, subject to safety constraints of the form $(x_{k+i}, y_{k+i}) \in \mathcal{S}_{\text{safe}}$ for all $y_{k+i} \in \mathcal{Y}_{k+i}$. Only the first control input is executed at each time step, and the process is repeated in a receding-horizon fashion.

This architecture enables long-horizon, uncertainty-aware planning while providing formal guarantees that the system will remain within a safe set with probability at least γ . Fig. 1 illustrates the overall pipeline of the proposed method. In this diagram, dark green dashed arrows represent Monte Carlo sampling used by the MPC controller to query whether a candidate control sequence leads to a safe trajectory under the current uncertainty tube—each query returns a Boolean feasibility result. Light green dashed arrows denote the loop over the prediction horizon $i = 1, \dots, T$, during which the conformal tube is propagated step-by-step using the calibrated uncertainty.

B. Dynamic Reachable Set Propagation

Given the current states x_k and y_k , suppose an open-loop candidate sequence of future control inputs $\mathbf{u}_{k:k+T-1} = u_k u_{k+1} \dots u_{k+T-1}$ is provided, for example, as part of a solution to an MPC optimization problem. Since the dynamics in (1) are deterministic, we can directly compute the resulting state trajectory $x_k x_{k+1} \dots x_{k+T}$ from the initial state x_k . Therefore, at each time step, our objective is to compute the reachable set of the uncontrollable agent, accounting for uncertainty through conformal prediction.

Definition 1 (Reachable Tube Generation): Suppose that, at each time step, the state of the controlled system x_{k+i} is known via open-loop prediction based on the given control sequence. For each $(x, y) \in \{x_{k+i}\} \times \mathcal{Y}_{k+i}$ where $\mathcal{A}(x_{k+i}, y_{k+i})$ is defined in (10), we define the unified uncertainty set over all possible $y \in \mathcal{Y}_{k+i}$ as:

$$\mathcal{A}(x_{k+i}, \mathcal{Y}_{k+i}) := \bigcup_{y \in \mathcal{Y}_{k+i}} \mathcal{A}(x_{k+i}, y). \quad (11)$$

The reachable set of the uncontrollable agent is then propagated as:

$$\mathcal{Y}_{k+i+1} = \bigcup_{\substack{y \in \mathcal{Y}_{k+i} \\ a \in \mathcal{A}(x_{k+i}, \mathcal{Y}_{k+i})}} g(y, a) \quad (12)$$

where we have $\mathcal{Y}_k = \{y_k\}$.

The above recursive formulation enables the dynamic construction of reachable tubes that incorporate prediction-time uncertainty about the uncontrollable agent's behavior, conditioned on the predicted trajectory of the controllable agent. These tubes can later be embedded into the MPC optimization as safety constraints.

C. Dynamic Tube MPC and Safety Guarantees

Given the current state $(x_k, y_k) \in \mathcal{S}_{\text{safe}}$ and a candidate control sequence $\mathbf{u}_{k:k+T-1}$, we use the open-loop predicted states $\{x_{k+i}\}_{i=0}^T$ of the controllable agent to condition the

Algorithm 1: Tube Generation and Safety Check

Input: Initial state x_t, y_t , control sequence $\{u_t, \dots, u_{t+T-1}\}$
Output: Safety flag `is_safe`

- 1 Compute trajectory $\{x_{t+\tau}\}_{\tau=1}^T$ using (1);
- 2 Compute reachable tube $\{\mathcal{Y}_{t+\tau}\}_{\tau=1}^T$ using (12);
- 3 `is_safe` \leftarrow True;
- 4 **for** $\tau = 1$ **to** T **do**
- 5 **if** $\exists y \in \mathcal{Y}_{t+\tau}$, s.t. $(x_{t+\tau}, y_{t+\tau}) \notin \mathcal{S}_{\text{safe}}$ **then**
- 6 `is_safe` \leftarrow False; **break**;
- 7 **return** `is_safe`

Algorithm 2: Tube-based MPC for Safety

Input: Current car state x_t , pedestrian state y_t
Output: Control input u_t for current time step

- 1 **foreach** candidate control sequence $u_t u_{t+1} \dots u_{t+T-1}$ **do**
- 2 Check safety using Algorithm 1;
- 3 **if** `is_safe` **then**
- 4 Evaluate cost $J = \sum_{\tau=1}^T \ell(u_{t+\tau-1}^r, u_{t+\tau-1})$;
- 5 Store feasible plan and cost;
- 6 **return** First control signal of the lowest-cost feasible plan

reachable tube propagation of the uncontrollable agent, as described in the previous section. The resulting sets $\{\mathcal{Y}_{k+i}\}_{i=0}^T$ represent the range of possible states of the uncontrollable agent at time $k+i$, under conformal prediction-based uncertainty.

We now formulate a finite-horizon T model predictive control (MPC) problem:

$$\min_{u_{k:k+T-1}} \sum_{i=0}^{T-1} \ell(u_{k+i}, u_{k+i}^r) \quad (13)$$

s.t. for any $i = 1, \dots, T$, we have

$$\begin{aligned} &x_k \text{ satisfies the dynamics of (1),} \\ &\{\mathcal{Y}_{t+\tau}\}_{\tau=1}^T \text{ is defined according to (12)} \\ &\forall y_{k+i} \in \mathcal{Y}_{k+i}, (x_{k+i}, y_{k+i}) \in \mathcal{S}_{\text{safe}}. \end{aligned}$$

Here, $\ell(\cdot)$ denotes the stage cost function, and \mathcal{Y}_{k+i} is the reachable set of the uncontrollable agent at time step $k+i$, computed based on conformal prediction uncertainty. The constraint enforces that the joint state remains within the safety set $\mathcal{S}_{\text{safe}}$ for all possible $y_{k+i} \in \mathcal{Y}_{k+i}$.

The MPC formulation above is implemented in Algorithm 2, which searches for a control sequence whose predicted evolution respects the safety constraint under worst-case reachable tubes. We emphasize that this work does not investigate explicit solutions to the optimization problem. Rather, we employ a simple Monte Carlo approach to heuristically identify feasible solutions that satisfy the safety constraints.

We now provide theoretical guarantees on the safety properties of the resulting control actions.

Theorem 1 (Stepwise Safety Guarantee): The safety guarantee step-wisely decays geometrically with a factor γ . Suppose $\mathbb{P}(y_{k+i} \in \mathcal{Y}_{k+i}) \geq \beta$ and $\mathcal{A}(\cdot)$ we get from (9), we have $\mathbb{P}(y_{k+i+1} \in \mathcal{Y}_{k+i+1}) \geq \gamma \cdot \beta$.

Proof: At time step $k+i$, given fixed $x = x_{k+i}$, for any y_{k+i} the agent's action satisfies $\mathbb{P}(a_{k+i} \in \mathcal{A}(x_{k+i}, y_{k+i}) \mid y_{k+i}) \geq \gamma$. By total probability:

$$\begin{aligned} &\mathbb{P}(a_{k+i} \in \mathcal{A}(x_{k+i}, \mathcal{Y}_{k+i})) \\ &= \int \mathbb{P}(a_{k+i} \in \mathcal{A}(x_{k+i}, y_{k+i}) \mid y_{k+i}) d\mathbb{P}(y_{k+i}) \\ &\geq \int_{\mathcal{Y}_{k+i}} \gamma d\mathbb{P}(y_{k+i}) \\ &= \gamma \cdot \mathbb{P}(y_{k+i} \in \mathcal{Y}_{k+i}) \geq \gamma \cdot \beta. \end{aligned}$$

\mathcal{Y}_{k+i+1} is propagated as defined in (12). Since we consider the worst cases and no additional uncertainty is introduced, $\mathbb{P}(y_{k+i+1} \in \mathcal{Y}_{k+i+1}) = \mathbb{P}(a_{k+i} \in \mathcal{A}(x_{k+i}, \mathcal{Y}_{k+i})) = \gamma \cdot \beta$. ■

Theorem 2 (Cumulative Safety Guarantee): Based on the current states x_k and y_k , under a control sequence given by (13), the probability that all constraints are satisfied over the entire horizon is lower bounded by:

$$\mathbb{P}\left(\bigcap_{i=1}^T (x_{k+i}, y_{k+i}) \in \mathcal{S}_{\text{safe}}\right) \geq \gamma^T. \quad (14)$$

Proof: The safety guarantee follows the geometrical decay of the safety probability with a factor of γ . Since the given initial state satisfies the safety constraint with probability $\mathbb{P}((x_k, y_k) \in \mathcal{S}_{\text{safe}}) = 1$, it follows that for any future time step $k+i$ ($i = 1, \dots, T$), we have

$$\mathbb{P}((x_{k+i}, y_{k+i}) \in \mathcal{S}_{\text{safe}}) \geq \gamma^i. \quad (15)$$

Note that, the above result provides the safety guarantee for the case if one applies the open-loop sequence for T steps. Yet, since our MPC in Algorithm 2 is executed in a receding horizon manner, the safety guarantee always remains at the probability γ . In asynchronous settings (computing the optimal control action may require non-negligible time) where control executes open-loop for i steps before replanning, the effective guarantee becomes γ^i . Our framework accommodates this by planning over extended horizons and ensuring safety under compounded probability.

Remark 2 (Comparison with other MPCs): In some other MPC formulations, joint chance constraints over a horizon are typically intractable. A common workaround is to apply Boole's inequality and enforce step-wise constraints, such as $\mathbb{P}[h(x_i, y_i) \leq 0] \geq 1 - \epsilon/T$ [15], though this often yields conservative results. In contrast, methods like [9] reformulate chance constraints as second-order cone constraints under Gaussian uncertainty, provided the mean and variance are convex functions of the state. However, in our setting, the uncertainty is predicted by a neural network, making the resulting mean and variance non-convex functions. This prevents direct convex reformulations and necessitates sampling-based evaluation in our MPC.

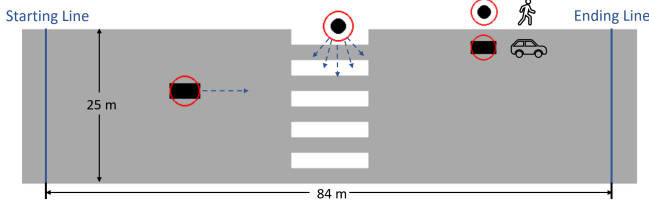


Fig. 2: The pedestrian’s walking logic is modeled as an unknown stochastic distribution affected by the state of the vehicle, i.e., $a \sim \mathcal{D}(x, y)$. Red circles indicate collision volume.

IV. SIMULATION AND RESULTS

In this section, we illustrate and evaluate the proposed approach through simulations of a case study involving autonomous driving with uncontrollable pedestrians. This case study demonstrates the effectiveness of our framework in managing the interactions between the autonomous vehicle and pedestrians, ensuring safety despite the uncertainty in pedestrian behavior. Our entire framework is implemented in Python and all codes are available in our project website.¹

A. Scenario Description and System Dynamics

Scenario Setup: As illustrated in Fig. 2, the scenario is set on a straight road segment with a total length of 84 m. A crosswalk is located within this segment, and the road has a width of 25 m. The starting line for the vehicle is positioned at one end of the road, while the ending line is at the opposite end. A pedestrian is present near the crosswalk, and a vehicle is approaching from the starting line.

Vehicle Dynamics: For the sake of simplicity, we assume the vehicle can move straight through a crosswalk, setting the dimension $n = 1$ with dynamic $v_{\text{car}} = u$. This assumption aligns with real-world constraints, as vehicles are generally not permitted to maneuver left or right while crossing a zebra crossing. Nevertheless, our approach naturally extends to two or higher dimensions. The vehicle’s speed $v_{\text{car}} \in [0, 15]$ m/s reflecting typical vehicle speeds observed in urban environments (up to the speed limit of $15 \text{ m}\cdot\text{s}^{-1}/54 \text{ km}\cdot\text{h}^{-1}/33 \text{ mph}$ in urban area).

Pedestrian Behavior: The external agent is modeled as a single-integrator system, where the control input is directly equal to the velocity in each direction for 2D senario. At each time step, the action $a_k \in \mathbb{R}^2$ is sampled from

$$a_k \sim \mathcal{D}(x_k, y_k) = \mathcal{N}_2(\phi(x_k, y_k), \Sigma).$$

Pedestrians’ actions always have internal logic but also randomness, thus a_k follows a Gaussian distribution whose mean is the nonlinear function function value $\phi(x, y)$ shown in Fig.4. $\phi(\cdot)$ captures the internal logic of pedestrian behavior at crosswalks, as the vehicle approaches at a higher speed, the pedestrian slows down in the direction perpendicular to the road, exhibiting more cautious crossing behavior. Simultaneously, the pedestrian’s velocity in the parallel direction increases, moving away from the vehicle as

an evasive response. And in simulation, we set the standard deviations of the action noise to be on the same order of magnitude as the typical pedestrian action in each dimension, i.e., $\Sigma = \text{diag}(\sigma_{\parallel}^2, \sigma_{\perp}^2) = ((0.5\text{m})^2, (0.1\text{m})^2)$.

Quick Passing and Collision Avoidance Task: The car needs to pass the intersection at a speed as close to the speed limit(15m/s) as possible while keeping a safe distance from pedestrians. The simulation continuously monitors the distance between the vehicle and the pedestrian, and our MPC is applied to synthesize safe control actions to avoid collisions.

Data Collection and Network Predictor: The dataset is generated by simulating a vehicle moving at a constant speed sampled from the uniform distribution $U[0, 15]\text{m/s}$, while tracking both the vehicle and pedestrian trajectories. The collected data is structured following the format described in Section II.B. The training dataset D_{train} contains 1×10^6 data, the testing dataset D_{test} contains 5×10^6 data and the calibration dataset D_{cal} for conformal prediction contains 2×10^5 data. We trained a feedforward neural network to predict the future actions of the pedestrian. The model consists of three fully connected layers with ReLU activation. The input layer maps features to 64 hidden units, followed by a second layer of 64 units, and a final output layer predicting pedestrian speed $(\hat{a}_{\parallel}, \hat{a}_{\perp}) \in \mathbb{R}^2$. The model use the Adam optimizer (learning rate 0.001) and MSE loss. A StepLR scheduler halves the learning rate every 10 epochs over 50 epochs.

Safety Set: For vehicle-pedestrian collision avoidance, We frame safety set $\mathcal{S}_{\text{safe}}$ as the 0-upper level set of a Lipschitz continuous function $h(x, y)$, i.e., $\mathcal{S}_{\text{safe}} = \{(x, y) \mid h(x, y) \geq 0\} \subseteq \mathbb{R}^{n_x} \times \mathbb{R}^{n_y}$, $h(x, y) = \|x - y\| - d_{\text{safe}}$. And our objective is to synthesize a safety filter for reference control at each time instant such that the controlled system can ensure safety with respect to the uncontrollable agent, with a certain level of confidence. Set $d_{\text{safe}} = 1.0 \text{ m}$, the collision volume is shown as the red circle in Fig. 2.

Conformal Regions and Reachable Tube Calculation:

To construct conformal regions, we partition the joint state space into $15 \times 3 \times 1 \times 2 = 90$ grid cells based on car speed (15 bins), predicted pedestrian perpendicular speed (3 bins), parallel speed (1 bin), and pedestrian position (2 bins). For each cell, we compute the $\gamma(=0.9)$ quantiles of the prediction errors in each action dimension to obtain conformal bounds $(\eta_{\parallel}, \eta_{\perp})$, using a calibration set of 20,000 samples.

Crucially, since the dynamics function g is component-wise monotonic, we can directly propagate the interval endpoints instead of computing the full set of possible next states. For more complicated systems without such monotonic structure, more general reachability tools such as *Taylor Models* ([27]) can be used to obtain tighter over-approximations.

Experiment Design: To evaluate the effectiveness of our approach, we compare the following five controllers in simulation. Given the current state x_k and y_k , for all $i \in [0, T]$:

- 1) **Tube MPC (Ours):** At each time step, we solve an MPC problem that maximizes car speed while ensuring

¹https://github.com/Yangming911/Conformal_Tube_MPC

Algorithm \ T	Success Rate			Average Speed [m/s]			Average Decision Time [ms]		
	1	10	20	1	10	20	1	10	20
Safety Tube MPC	34.9%	84.8%	98.6%	14.98	14.92	14.89	400.745	3365.504	6888.803
Vanilla MPC	33.5%	49.4%	75.9%	15.03	14.96	14.93	161.875	2384.445	4580.410
Safety Region CBF	75.4%	72.3%	71.4%	14.85	14.66	14.67	134.257	1108.849	2217.946
Vanilla CBF	67.7%	74.0%	71.1%	14.89	14.74	14.74	139.781	1020.415	1996.130
Baseline(Constant Speed)	31.8%			15.03			-		

TABLE I: Success rate, average speed and average decision time for our conformal tube MPC compared to other methods.

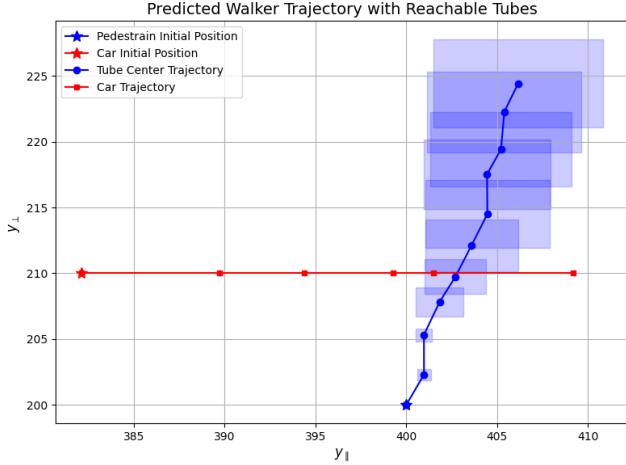


Fig. 3: An example that does not meet the safety constraint under our approach. The blue boxes indicate the pedestrian's conformal reachable tube generated via (12). The car enters pedestrian reachable tube when $T = 4$.

safety over a T -step horizon, but only apply the first control in the optimal sequence. Given the predicted pedestrian reachable tube \mathcal{Y}_{k+i} generated by (12), the safety constraint is: $\forall y_{k+i} \in \mathcal{Y}_{k+i}, (x_{k+i}, y_{k+i}) \in \mathcal{S}_{\text{safe}}$. Fig. 3 shows an example that does not satisfy the safety constraint under this approach. The car and pedestrian access pipes do not maintain a safe distance when $T=4$.

- 2) **Vanilla MPC**: A standard MPC controller that plans over a T -step horizon without modeling uncertainty. No conformal region is used, and only one predicted pedestrian trajectory $\{\hat{a}_{k+i}\} = \Omega(x_{k+i}, \hat{y}_{k+i}|\theta), \{\hat{y}_{k+i}\} = g(y_{k+i-1}, \hat{a}_{k+i-1})$ is considered. The safety constraint requires all predicted states to satisfy $(x_{k+i}, \hat{y}_{k+i}) \in \mathcal{S}_{\text{safe}}$.
- 3) **CP + CBF**: A trajectory-level Control Barrier Function (CBF) controller adapted from [28] that incorporates uncertainty via conformal prediction. Similar as Vanilla MPC, we do not propagate the conformal region forward across time. At each time step, we use the conformal region $\mathcal{A}(x_{k+i}, \hat{y}_{k+i})$ to construct a only one-step reachable set \mathcal{Y}_{k+i} and the safety constraint is: $\forall y_{k+i} \in \mathcal{Y}_{k+i}, (x_{k+i}, y_{k+i}) \in \mathcal{S}_{\text{safe}}$.
- 4) **Vanilla CBF**: A baseline CBF controller without uncertainty modeling. The CBF constraint is applied directly to $\{\hat{y}_{k+i}\}$, and the safety constraint requires all predicted states to satisfy $(x_{k+i}, \hat{y}_{k+i}) \in \mathcal{S}_{\text{safe}}$.
- 5) **Constant Speed(15 m/s)**: The car crashes into zebra

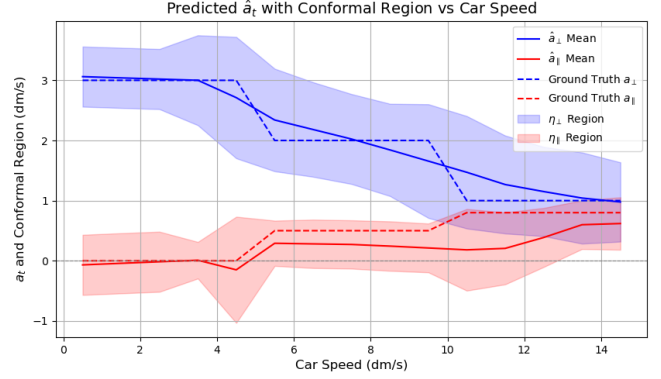


Fig. 4: Pedestrian behavior predicted by neural networks. The plot also includes $\phi(\text{car speed})$ with all other parameters(the position and velocity of pedestrian, the position of the car) fixed as a noise-free reference ground truth, while the shaded regions show calibrated uncertainty at confidence level $\gamma = 0.85$

crossing at constant speed without any feedback or safety constraint.

B. Results

We evaluate the proposed conformal tube MPC framework in a pedestrian-vehicle interaction scenario. The vehicle aims to maintain high speed while avoiding collisions with a pedestrian whose actions are uncertain and coupled to the vehicle's state.

Fig. 4 shows the how the network learns the underlying random distribution governing pedestrian behavior in relation to the vehicle's state. Notably, our method does not rely on the precise accuracy, overall performance, or scene comprehension capabilities of the model, making it robust to model imperfections and uncertainties. The predicted conformal bounds adapt to different car speeds and align closely with the ground truth $\phi(\cdot)$, demonstrating accurate and uncertainty-aware behavior modeling.

Quantitative comparisons across five baseline methods (Table I) show that our method achieves the highest safety success rate, especially for larger planning horizons. At $T = 20$, our approach attains over 91% success, significantly outperforming vanilla MPC and CBF-based controllers. This confirms the advantage of propagating uncertainty-aware reachable tubes across the planning horizon, rather than relying on single-step or deterministic predictions.

Moreover, while Safety Tube MPC incurs higher computational cost due to recursive reachable set computation and Monte Carlo sampling (6.889s at $T = 20$), it remains suitable for high-assurance applications where safety is critical. These

results validate the practical benefits of integrating conformal prediction with dynamic reachability and MPC for safe planning under coupled agent uncertainty.

V. CONCLUSION AND DISCUSSIONS

This work presents a safety assurance framework that integrates tube model predictive control with conformal prediction for systems operating alongside uncontrollable agents. The proposed approach addresses state-action coupling between controlled and uncontrolled agents while providing probabilistic safety guarantees. Note that this work uses a simple Monte Carlo method to solve the MPC problem with reachable tubes. As discussed in Remark 2, more efficient alternatives may be possible if the neural network predictor can be approximated in a tractable form. For example, recent works have explored convex reformulations under structural assumptions [29], enabling integration into optimization-based controllers. Exploring such techniques for control-aware neural approximations is a promising direction for future work. These directions are inspired by robust MPC and risk-sensitive control frameworks and may lead to more scalable and real-time-capable solutions. Additionally, one limitation of our current approach is the assumption that precise state information for both the controlled system and the uncontrollable agent is fully accessible. In many practical applications, such state information must be obtained through perception devices like LiDAR, which can introduce estimation errors. To address this, we plan to extend our framework to perception-based settings, incorporating techniques to handle state estimation uncertainty and further improve the robustness of our approach in real-world scenarios.

REFERENCES

- [1] B. Paden, M. Čáp, S. Z. Yong, D. Yershov, and E. Frazzoli, “A survey of motion planning and control techniques for self-driving urban vehicles,” *IEEE Transactions on Intelligent Vehicles*, vol. 1, no. 1, pp. 33–55, 2016.
- [2] S. Lefèvre, D. Vasquez, and C. Laugier, “A survey on motion prediction and risk assessment for intelligent vehicles,” *Robotics and Autonomous Systems*, vol. 58, no. 9, pp. 1372–1394, 2014.
- [3] A. Kim, S. Lee, J. Choi, S. Oh, C. Choi, S. Lee, J. Choi, S.-W. Choi, and S. Lee, “Social interactions for autonomous driving: A review and perspective,” *Foundations and Trends® in Machine Learning*, vol. 16, no. 1, pp. 1–80, 2023.
- [4] D. Sadigh, S. S. Sastry, S. A. Seshia, and A. D. Dragan, “Planning for autonomous cars that leverage effects on human actions,” in *Robotics: Science and Systems XII*, 2016.
- [5] J. F. Fisac, E. Bronstein, E. Stefansson, D. Sadigh, S. S. Sastry, and A. D. Dragan, “Hierarchical game-theoretic planning for autonomous vehicles,” *arXiv preprint arXiv:1903.00640*, 2019.
- [6] X. Wang, Z. Li, Y. Zhang, Y. Zhang, and J. Liu, “S4tp: Social-suitable and safety-sensitive trajectory planning for autonomous vehicles,” *IEEE Transactions on Intelligent Vehicles*, 2024.
- [7] D. Q. Mayne, M. M. Seron, and S. V. Raković, “Robust model predictive control: A survey,” *Automatica*, vol. 41, no. 12, pp. 2199–2231, 2005.
- [8] A. Nilim and L. El Ghaoui, “Robust control of markov decision processes with uncertain transition matrices,” *Operations Research*, vol. 53, no. 5, pp. 780–798, 2005.
- [9] L. Blackmore, M. Ono, and B. C. Williams, “Chance-constrained optimal path planning with obstacles,” in *IEEE Transactions on Robotics*, vol. 27, no. 6. IEEE, 2011, pp. 1080–1094.
- [10] N. Rhinehart, R. McAllister, and S. Levine, “Precog: Prediction conditioned on goals in visual multi-agent settings,” *Proceedings of the IEEE/CVF International Conference on Computer Vision*, pp. 2821–2830, 2019.
- [11] S. Casas, C. Gulino, R. Liao, and R. Urtasun, “Implicit latent variable model for scene-consistent motion forecasting,” in *Proceedings of the European Conference on Computer Vision*. Springer, 2020, pp. 624–641.
- [12] S. Ejaz and M. Inoue, “Trust-aware safe control for autonomous navigation: Estimation of system-to-human trust for trust-adaptive control barrier functions,” *arXiv preprint arXiv:2307.12815*, 2023.
- [13] A. N. Angelopoulos and S. Bates, “A gentle introduction to conformal prediction and distribution-free uncertainty quantification,” *arXiv preprint arXiv:2107.07511*, 2021.
- [14] J. Sun, Y. Jiang, J. Qiu, P. Nobel, M. J. Kochenderfer, and M. Schwager, “Conformal prediction for uncertainty-aware planning with diffusion dynamics model,” *Advances in Neural Information Processing Systems*, vol. 36, 2024.
- [15] L. Lindemann, M. Cleaveland, G. Shim, and G. J. Pappas, “Safe planning in dynamic environments using conformal prediction,” *IEEE Robotics and Automation Letters*, vol. 8, no. 8, pp. 5116–5123, 2023.
- [16] S. Yang, G. J. Pappas, R. Mangharam, and L. Lindemann, “Safe perception-based control under stochastic sensor uncertainty using conformal prediction,” in *2023 62nd IEEE Conference on Decision and Control (CDC)*. IEEE, 2023, pp. 6072–6078.
- [17] R. Ivanov, T. J. Carpenter, J. Weimer, R. Alur, G. J. Pappas, and I. Lee, “Verifying the safety of autonomous systems with neural network controllers,” *ACM Trans. Embed. Comput. Syst.*, vol. 20, no. 1, Dec. 2020.
- [18] T. Waite, Y. Geng, T. Turnquist, I. Ruchkin, and R. Ivanov, “State-dependent conformal perception bounds for neuro-symbolic verification of autonomous systems,” 2025.
- [19] A. Dixit, L. Lindemann, S. X. Wei, M. Cleaveland, G. J. Pappas, and J. W. Burdick, “Adaptive conformal prediction for motion planning among dynamic agents,” in *Learning for Dynamics and Control Conference*. PMLR, 2023, pp. 300–314.
- [20] G. Shafer and V. Vovk, “A tutorial on conformal prediction,” *Journal of Machine Learning Research*, vol. 9, no. 3, 2008.
- [21] V. Vovk, A. Gammernan, and G. Shafer, “Algorithmic learning in a random world,” *Algorithmic Learning in a Random World*, 01 2005.
- [22] M. Fontana, G. Zeni, and S. Vantini, “Conformal prediction: A unified review of theory and new challenges,” *Bernoulli*, vol. 29, no. 1, Feb. 2023.
- [23] J. Lei, M. G’Sell, A. Rinaldo, R. J. Tibshirani, and L. W. and, “Distribution-free predictive inference for regression,” *Journal of the American Statistical Association*, vol. 113, no. 523, pp. 1094–1111, 2018.
- [24] R. J. Tibshirani, R. Foygel Barber, E. Candès, and A. Ramdas, “Conformal prediction under covariate shift,” *Advances in neural information processing systems*, vol. 32, 2019.
- [25] V. Vovk, “Conditional validity of inductive conformal predictors,” in *Proceedings of the Asian Conference on Machine Learning*, ser. Proceedings of Machine Learning Research, S. C. H. Hoi and W. Buntine, Eds., vol. 25. Singapore Management University, Singapore: PMLR, 04–06 Nov 2012, pp. 475–490.
- [26] I. Gibbs and E. Candès, “Adaptive conformal inference under distribution shift,” *arXiv preprint arXiv:2106.00170*, 2021.
- [27] K. Makino and M. Berz, “Taylor models and other validated functional inclusion methods,” *International Journal of Pure and Applied Mathematics*, vol. 6, pp. 239–316, 2003.
- [28] S. Wang, S. Li, and X. Yin, “Sparc: Prediction-based safe control for coupled controllable and uncontrollable agents with conformal predictions,” 2024.
- [29] Y. Chen, Y. Shi, and B. Zhang, “Optimal control via neural networks: A convex approach,” 2019.